Research Article

pISSN: 2345-5357
eISSN: 2423-4214

APPLIED FOOD BIOTECHNOLOGY, 2022, 9 (4):275-286
Journal homepage: www.journals.sbmu.ac.ir/afb

OPEN ACCESS

Biosynthesis of Nano-Calcite and Nano-Hydroxyapatite by the Probiotic Bacteria of *Bacillus subtilis* and *Bacillus coagulans*

Sabere Nouri, Rasoul Roghanian*, Giti Emtiazi, Rasoul Shafiei

Department of Cell and Molecular Biology and Microbiology, Faculty of Biological Science and Technology, University of Isfahan, Isfahan, Iran.

Abstract

Background and Objective: In recent years, green synthesis of nanobiomaterials has received more attentions than chemical synthesis due to their ecofriendly and compatibility. The aims of this study were to investigate synthesis of nanobiomaterials from probiotics and characterize these nanobiomaterials.

Material and Methods: *Bacillus subtilis* and *Bacillus coagulans* were cultured in media containing insoluble calcium phosphate and urea, and produced nano-hydroxyapatite and nano-calcite. Productions were surveyed in three stages. First, produced particles were assessed on the surface of the dried bacteria at room temperature. In the second stage, dried bacteria were burned at 600 ºC. In the final stage, hydroxyapatite was purified using nanofilters. Characterization and elemental analysis of the biomaterials were studied using Fourier transform infrared spectroscopy, X-ray diffraction, scanning electron microscopy, ultraviolet-visible spectroscopy, energy dispersive X-ray and X-ray fluorescence.

Results and Conclusion: It was shown that nano-calcite and braided nano-hydroxyapatite on the dried biomass surface and nano-hydroxyapatite were made only in media containing insoluble calcium phosphate supplemented by urea, which was induced by phosphatase and urease. Removing organic matters by heat treatment led to the further purity of the particles. The X-ray fluorescence results revealed purity of the nano-hydroxyapatite, which was achieved by filtration of particles after burning. The ratio of calcium to phosphorus in *B. coagulance* sample reached 1.8, which was close to stoichiometric hydroxyapatite. Since nanobiomaterials are made from probiotics, these particles can be appropriate candidates to use in food industries, sanitation and medicine. Braided nano-hydroxyapatite can substitute needle-like types of food additives for infants and elderly people because of its safety.

Conflict of interest: The authors declare no conflict of interest.

Article Information

Article history:
- Received 3 June 2022
- Revised 18 July 2022
- Accepted 30 July 2022

Keywords:
- *Bacillus coagulans*
- *Bacillus subtilis*
- Calcite
- Food additive
- Hydroxyapatite
- Probiotic

***Corresponding author:**

Rasoul Roghanian
Department of Cell and Molecular Biology and Microbiology, Faculty of Biological Science and Technology, University of Isfahan, Isfahan, Iran.

Tell: +989131170669
Fax: +98-31-36687396

E-mail:
rasoul_roghanian@yahoo.co.uk

How to cite this article

Nouri S, Roghanian R, Emtiazi G, Shafiei R. Biosynthesis of Nano-Calcite and Nano-Hydroxyapatite by the Probiotic Bacteria of Bacillus subtilis and Bacillus coagulans. Appl Food Biotechnol. 2022; 9 (4): 275-286. http://dx.doi.org/10.22037/afb.v9i4.38768

1. Introduction

Calcium phosphate salts are the major mineral components of vertebrate bones and teeth. Nearly 70% of the bones are made up of the biomineral phase, majorly composed of one or more calcium phosphate molecules [1]. Of the calcium phosphate salts, hydroxyapatite (HA) [$Ca_{10}(PO_4)_6(OH)_2$] is the most analogous to the mineral components of the bones since it is the most thermody--namically stable crystalline form of calcium phosphate in body fluids [2]. Moreover, calcite is an abundantly available material that includes significant medical uses; in particular, it can strengthen bones as well as filling them [1,2]. Studies have been carried out on HA for various biomedical reasons such as tissue engineering, dental implanting, implant coating and bone grafting [3]. Other critical uses of HA include drug delivery systems [3], sunscreen agents [4] and toothpastes [5]. Furthermore, HA and calcite are food additives and nutritional supplements. In previous studies, active edible coatings containing HA and calcite have been

used to extend the food shelf-life [6]. Moreover, these compounds are used as food supplements to absorb further iron and as calcium supplies [7]. Since one of the factors in dental erosion is consumption of acidic soft drinks, HA additives are used in acidic soft drinks to prevent tooth decays. Moreover, HA nanoparticles are used in soft drinks to prevent erosion [8]. One of the most important uses of these two biomaterials in industries includes addition of these biomaterials to chewing gums for better teeth protection [5,9], infant formulas and elderly people food supplements [10,11]. Nanotechnology is a multidisciplinary scientific area, which uses a diverse array of tools and techniques derived from engineering, physics, chemistry and biology [12-14]. Advancements in nanoscience and nanotechnology have made it possible to manufacture and characterize submicron bioactive carriers. Delivery of bioactive materials to target sites insides the body and their release behaviors are directly affected by the particle size [15]. Compared to micrometer-sized carriers, nanocarriers provide further more surface areas and include the potential to increase solubility, enhance bioavailability, improve controlled release and enable precision targeting of the entrapped materials to greater extents [13,16].

Several chemical methods are available for synthesizing HA, including solid-state reaction, mechanochemical reaction, spark plasma system, alkali-acid process, sol-gel process, sonochemical process, microwave-assisted process, multiple emulsion technique, precipitation technique, plasma spraying system and hydrothermal, conversion and solution combustion methods [17,18]. Use of several chemicals to achieve a controlled synthesis is common in these processes, although the produced nanomaterials are often toxic [17,19]. In recent years, the green synthesis has become popular, considering all aspects of chemical synthesis as they are ecofriendly, less expensive and easier to achieve. The present nanobiotechnology focuses on environmentally friendly biosynthetic processes; in which, microorganisms demonstrate potentials for nanosynthesis biomanufacturing devices [20]. Green HA sources include bone tissues from most animals such as poultries and fishes, corals, shrimp shells, snakeskins, hedgehog thorns, plants, fungi and algae [18,21,22]. One of the green methods of synthesis of nano-HA is biomineralization by bacteria, which includes several advantages over other processing methods. However, a few studies have been carried out on this method [19,21]. Bacteria, including *Serratia marcescens*, and *Alkanindiges illinoisensis*, have been shown to synthesize HA [21,22]. Ability of biological processes to control form, phase, orientation and nanostructural topography of the inorganic crystals is known as biomineralization [19,21,22]. Probiotics are technically economical and environmentally safe and cover a wide spectrum in medicine, food and drug industries. During the production and optimization of probiotic biosynthesis, ease of mass manufacturing, safety of handling probiotics and their importance for humans are important issues [23]. Production of nano-HA by probiotics as an antibacterial is safe for adding to foods to enhance general health while its effectiveness has not been reported. Therefore, the aim of this study was to synthesize nano-calcite and braided nano-HA by probiotics such as *Bacillus* (*B.*) *subtilis* and *B. coagolance* to use in the food industry.

2. Materials and Methods

2.1. Materials and equipment

Materials: Nutrient agar, dextrose, $Ca_3(PO_4)_2$, NaCl, KCl, $MgSO_4.7H_2O$, yeast extract, $FeSO_4.7H_2O$, $MnSO_4 \cdot H_2O$ and agar-agar (Merck, Germany), and *p*-nitrophenyl phosphate (Sigma-Aldrich, USA).

Equipment: Furnace (Nabertherm, Germany), X-ray diffraction (XRD) (D8 Advance, Bruker, Germany), Fourier transform infrared spectroscopy (FTIR) (JASCO FT/IR-6300, Japan), scanning electron microscopy (SEM) (Philips XI30, the Netherlands), ultraviolet-visible-near-IR (UV-vis) spectrophotometry (JASCO V_670, Japan), energy-dispersive X-ray (EDX) (Philips XI30, the Netherlands), X-ray fluorescence spectroscopy (XRF) (S4-Pioneer, Germany), microcentrifuge (Hettich, Germany), and spectrophotometry (Spectronic 21D, USA).

2.2. Cultivation of bacteria and biosynthesis of nano-inorganic materials

In this study, standard probiotic bacterial strains of *B. coagulans* ATCC 7050 (Iranian Biological Resource Center, Tehran, Iran) and *B. subtilis* PTCC 1204 (Persian Type Culture Collection, Tehran, Iran) were used for nanoparticle production. These two strains were cultured separately on nutrient agar media after heat shock and incubated at 37 °C for 24 h. Then, the strains individually were spread plate cultured on Pikovskaya (PVK) media and 0.1% urea as well as PVK media alone. The PVK media included (g l^{-1}) dextrose 10, $Ca_3(PO_4)_2$ 5, NaCl 0.2, KCl 0.2, $MgSO_4.7H_2O$ 0.1, yeast extract 0.5, $FeSO_4.7H_2O$, 0.002, $MnSO_4 \cdot H_2O$, 0.002 and agar-agar 15 (pH 7.2) [22]. The potential of these two bacteria for the production of calcite and HA was verified by investigating clear zones on the PVK media. Utilizing insoluble tricalcium phosphate by the bacteria and phosphatase activities induced clear zones around the culture lines. After five days, cultured strains were harvested from the surface of the PVK agar plate using loops and dried in fresh plates for 1 h at room temperature (25-30 °C). Production of nanoparticles by the probiotics cultured in media containing urea and tricalcium phosphate was carried out in three stages. First, production of these particles was studied on the surface of the dried bacteria and then dried bacteria were sintered at 600 °C for 2 h. Then, HA was purified using nanofilters. The achieved powder (dried and sintered samples) was characterized.

2.3. Identification of nano-inorganic particles

Powder samples were identified using XRD at 35 kV and 30 mA in reflection mod with Cu Kα (λ = 1.540598 Å) radiation before and after purification of the synthesized powder. By a scanning speed of 0.04 s^{-1}, XRD data were collected in 2θ range of 10-80°. Chemical functional groups of the synthesized powder were investigated using FTIR spectra. All spectra were generated in a chemical bond absorption range of 350-4000 cm^{-1}. Morphology of all powder samples was investigated using SEM analyses at 20 kV. Gold sputtering (15-nm thickness) was carried out to cover the samples before the assessments. Diffusive reflective UV-vis measurement of the samples was carried out using UV-vis spectrophotometer at 2200-220 nm [4,18,19,21,22].

2.4. Assessment of calcium to phosphorus ratio of synthesized nanoparticles

The EDX analysis was used to investigate elemental compositions of the samples at 20 kV. Before the assessment, all samples were gold-sputtered with 15-nm thickness. The XRF spectroscopy was used to investigate elemental chemical compositions of the samples to assess rates of calcium to phosphorus (Ca: P) and other elements in the synthesized powder (the analysis ranges of fluorine to uranium) [18,19,21,22].

2.5. Enzyme assay

For the measurement of alkaline phosphatase (ALP) enzyme activity, strains were cultured in PVK broth, PVK and urea broth, and nutrient broth for five days. Samples were centrifuged at 4000 ×g for 20 min using microcentrifuge and the cell-free supernatants were collected for the assessment of ALP activity. The supernatant (10 µl) was mixed with 100 µl of the phosphatase enzyme reagent and incubated at 37 °C for 1 h. For preparing the ALP enzyme reagent, 7.6 mM of *p*-nitrophenyl phosphate solution were mixed with 100 mM Tris buffer (pH 10). Reaction was stopped by adding 100 µl of 0.5M NaOH and solution absorbance was measured at 405 nm using spectrophotometer. Quantity of the enzyme needed to liberate 1 µmol of *p*-nitrophenol per minute under assessment conditions was assessed as one unit of enzyme activity [24]. For the urease test, bacteria were cultured on urea-base agar media to assess their urea degradability by the urease. Bacteria that break down urea produced ammonia, which alkalinized the environment and turned the phenol-red reagent in the culture media to pink [24]. All assessments were carried out in three replications.

3. Results and Discussion

3.1. Biosynthesis of nano-inorganic materials

Potentials of *B. coagulans* and *B. subtilis* strains for the production of calcite and HA were assessed by investigating clear zones on the PVK media. Bacteria utilized insoluble tricalcium phosphate and phosphatase activities resulted in clear zones which shown in Figure S1 (a & b). Yields of nano-calcite and nano-HA after drying and sintering included 10 and 1 mg g-1 harvested biomass, respectively.

3.2. Characterization and identification of nano-inorganic particles

3.3. The X-ray diffraction analysis

The XRD pattern and structural analysis of the dried *B. coagulans* and *B. subtilis* biomasses from PVK media (without urea) are shown in Figure 1, revealing calcite peaks. However, XRD patterns of the cells cultured on PVK and urea demonstrated formation of calcite and HA (Figure 2). Calcite-linked peaks were seen at 2θ of 23, 29, 36, 39, 43 and 47, which were standard peaks of calcite [22,25] (Figures 1 and 2).

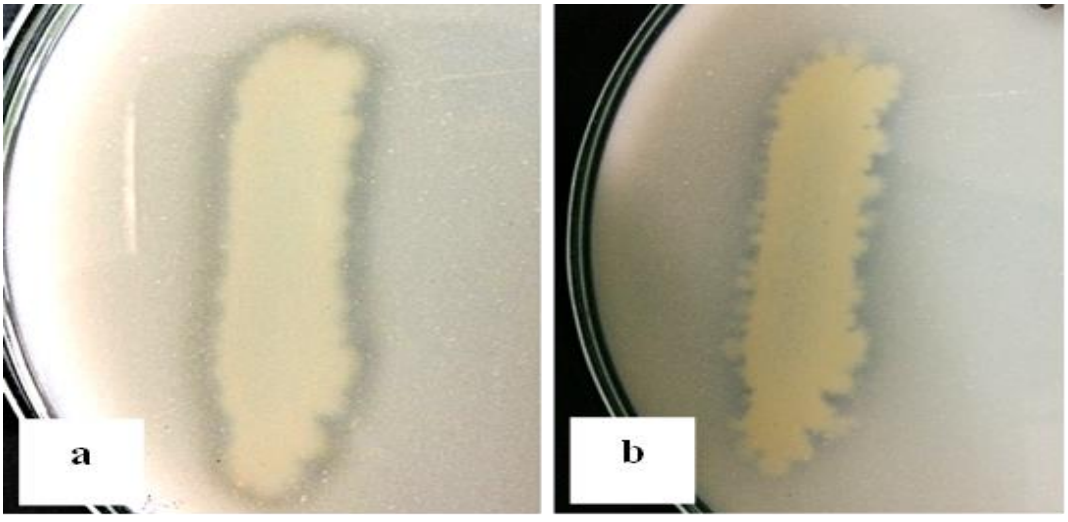

Figure 1S: Colonies of **(a)** *Bacillus coagulans* and (**b**) *Bacillus subtilis* on Pikovskaya media with clear zones, indicating use of insoluble tricalcium phosphate by the bacteria

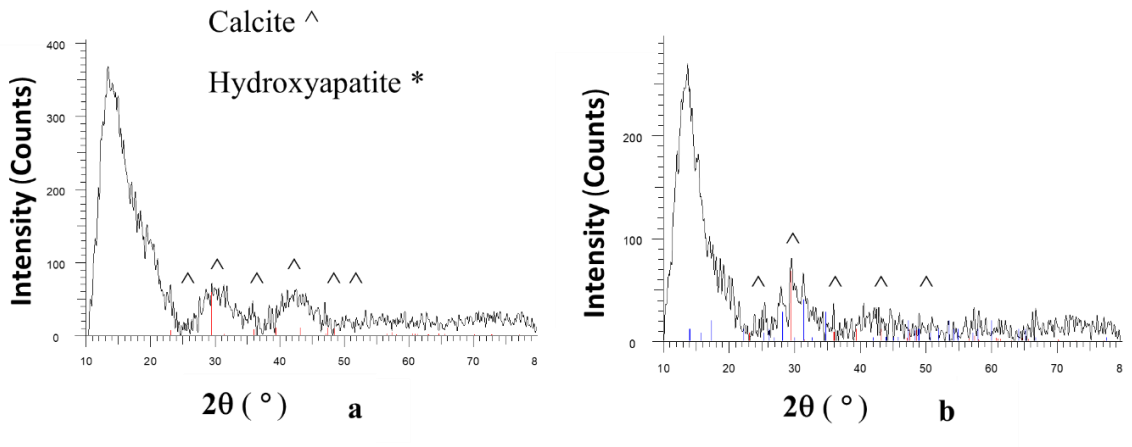

Figure 1. The X-ray diffraction patterns of the cultured samples on Pikovskaya, dried (a) *Bacillus coagulans* and (b) *Bacillus subtilis* masses

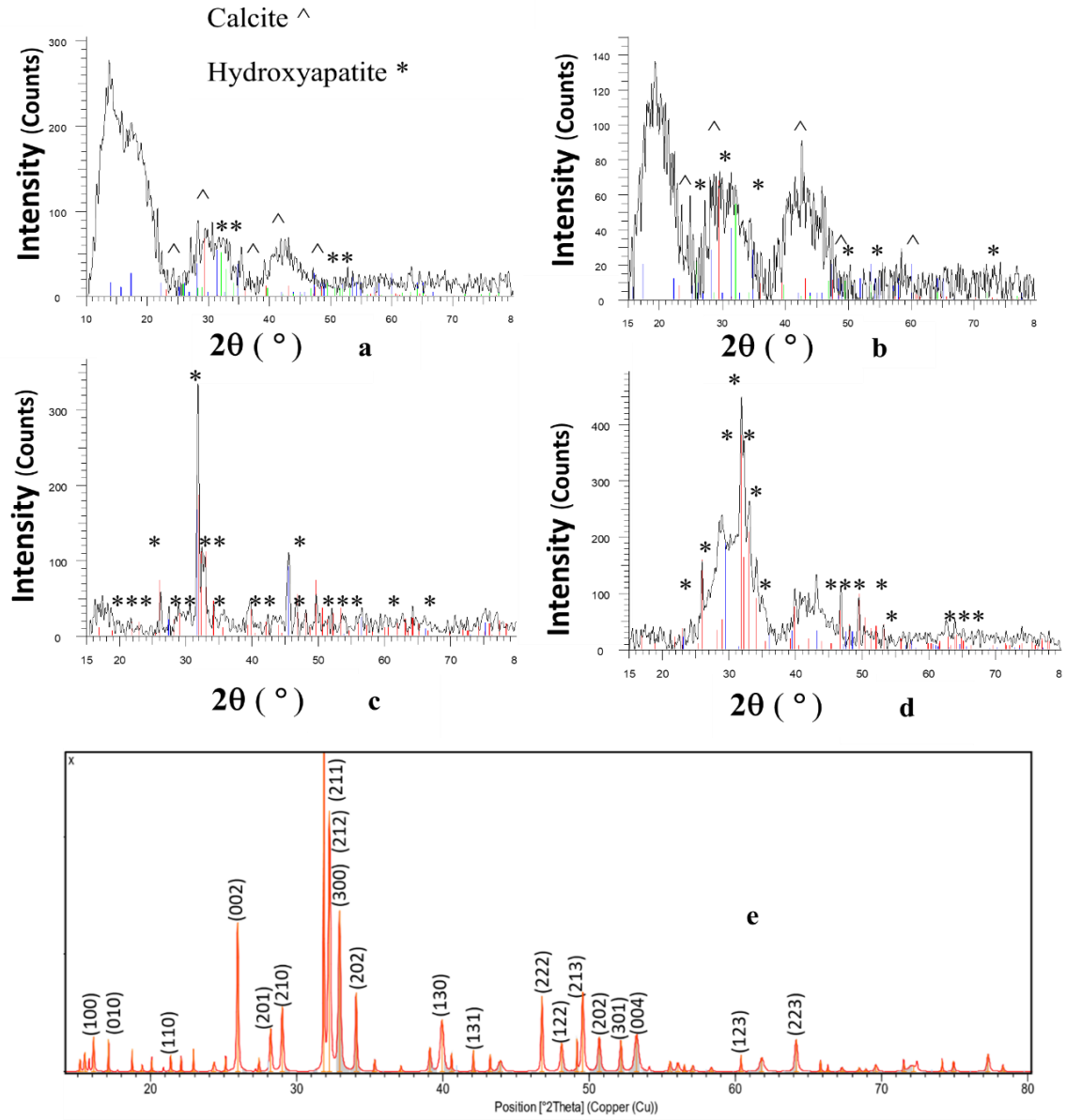

Figure 2. The X-ray diffraction patterns of the cultured samples on Pikovskaya and urea; dried (**a**) *Bacillus coagulans* and (b) *Bacillus subtilis* mass, sintered (**c**) *Bacillus coagulans*, (d) *Bacillus subtilis* at 600 ºC, and **(e)** ICDD database of standard peaks for hydroxyapatite with hkl numbers

Thus, addition of urea to the media did not include effects on calcite production. However, urea was necessary for the synthesis of HA. The XRD pattern of HA from dried *B. coagulans* and *B. subtilis* compared to the standard references (Figure 2e) in the International Centre for Diffraction Data (ICDD) file for HA (09-0432) are shown in Figures 2 (a,b). Samples were heated to decompose the calcite particles and organic debris to calcium oxide and carbon dioxide at 600 ºC for 2 h. After burning and removing organic matter and calcite, a cleaner peak of bio-HA was observed (Figures 2 c and d).

These data were similar to those of chemical HA production by burning *β*-tricalcium phosphate at temperatures greater than 600 °C [26]. Crystallinity of the synthesized HA was verified by the preferred orientation in 211 and 212 levels [18,26]. Other factors in probiotic bacteria such as organic matters were responsible for unlinked HA and calcite peaks in graphs (Figures 2a and b). Using Scherer equation, size of the crystals was calculated based on the XRD peaks and the HA and calcite sizes were nearly less than 100 nm. Although studies have shown that bacteria such as *S. marcescens*, and *A. illinoisensis* can mediate synthesis of HA [21,22,27], no studies have used probiotics to produce such biomaterials. As previously reported, calcite could be produced from *B. megaterium* in PVK media without urea [22]. Identifying peaks of HA and calcite formed by probiotics before purification qualifies them for use in food industries. Based on the previous findings, probiotics and HA are added separately to the soft drinks for antibacterial efficacy and tooth decay prevention, respectively [8,28]. Although probiotic chewing gums for general health [29] and HA chewing gums for protecting teeth [9] were addressed in previous studies, the current study revealed that addition of HA producing probiotics to chewing gums meets the two criteria. Contrary to the classical chemical methods, microbial HA and calcite particles could be produced with no heat, pressure and pH treatments. Burning was carried out only to purify HA from calcite and other organic materials.

3.3.1. Fourier transform infrared spectroscopy analysis

The FTIR spectra biosynthesized nano-HA particles from probiotic bacteria are shown in Figure 3. In fact, PO_4^{3-}, OH^-, Ca^{2+} and H_2O are the active chemical groups in HA and calcite particles [30] and HA and calcite particle characteristic absorption peaks are shown in Figure 3 (a and b).The FTIR of the nano-HA from *B. coagulans* and *B. subtilis* showed high absorption peaks at 3427.85 cm^{-1} (OH-stretching), which was supported by the previous studies [31]. Stretching modes of the P-O bonds in HA were correlated to the peaks of 1000-1100 cm^{-1}. Peaks in 560–606 cm^{-1} range occurred by bending modes of P-O bonds in the phosphate group. At 472, 567, 570, 605, 606, 960 and 965 cm^{-1}, typical peaks of the structure of PO_4^{3-} tetrahedral apatite were clearly shown. Carbonate groups of the $CaCO_3$ portion of HA were represented by characteristic bands nearly 1420 cm^{-1} in the two synthesized nano-HA particle. Bands of 1622 and 1629 cm^{-1} corresponded to the adsorbed H_2O. All bounds included similarities to the standard peaks of HA from chemical synthesis and biological synthesis from bovine bones [30,31].

3.3.2. Scanning electron microscope analysis

The SEM micrographs were used to assess sample particle sizes and morphological features as shown in Figure 4 (a and b). Particle sizes were less than 100 nm, depending on the graphs and the scale was similar to that on the nanoscale HA from human bones [32]. Nano-HA samples synthesized in this study showed that the particles included a uniform morphology in nanometer dimensions and showed that crystal growth in bacteria was uniform and braided as well; similarl to the previous studies for braided HA in bone structure [33]. Additionally, braided or woven bone was the first bone formed during initial bone formation in fracture and pathologic circumstances [33,34]. Synthesized HA from bacteria in other studies was almost spherical or tubular [21,22]. Various forms of HA additives are used in food industries such as baby formulas containing needle-like nanoparticles [10]. However, European Union Scientific Committee on Consumer Safety refuted this product by presenting documents, showing that use of needle-like HA nanoparticles in infant formulas was toxic and could be dangerous for infants. Up-to-date, there is no report on the toxicity of using woven or braided forms of HA produced in this study [10,35]. To the best of the authors' knowledge, this is the first report on biosynthesized braided nano-HA from probiotic bacteria (*B. coagulans* and *B. subtilis*) that could mimic the bone structure.

3.3.3. Ultraviolet-visible-near-IR spectroscopy

Characteristic absorbance wavelength of the samples was assessed using UV-vis spectroscopy. Diffuse reflectance of the synthesized nano-HA is shown in Figures 5a,b. Based on the previous studies, the optical absorption of pure HA in the UV region is 200-340 nm [36]. In this study, the two UV spectra of the synthesized nano-HA from *B. coagulans* and *B. subtilis* were nearly similar, with optical absorption in the UV range of 200-350 nm and a strong band below 250 nm. Results showed high transmittance zones at longer wavelengths, which were interesting for optical limiting due to their better transparency for weak lights. No evidence are available reporting UV for bacterial HA nanoparticles. However, HA extracted from natural sources (plants) included similar analysis results to the results of the present study. The UV analysis of the chemical samples was similar to that of the present study [4,36].

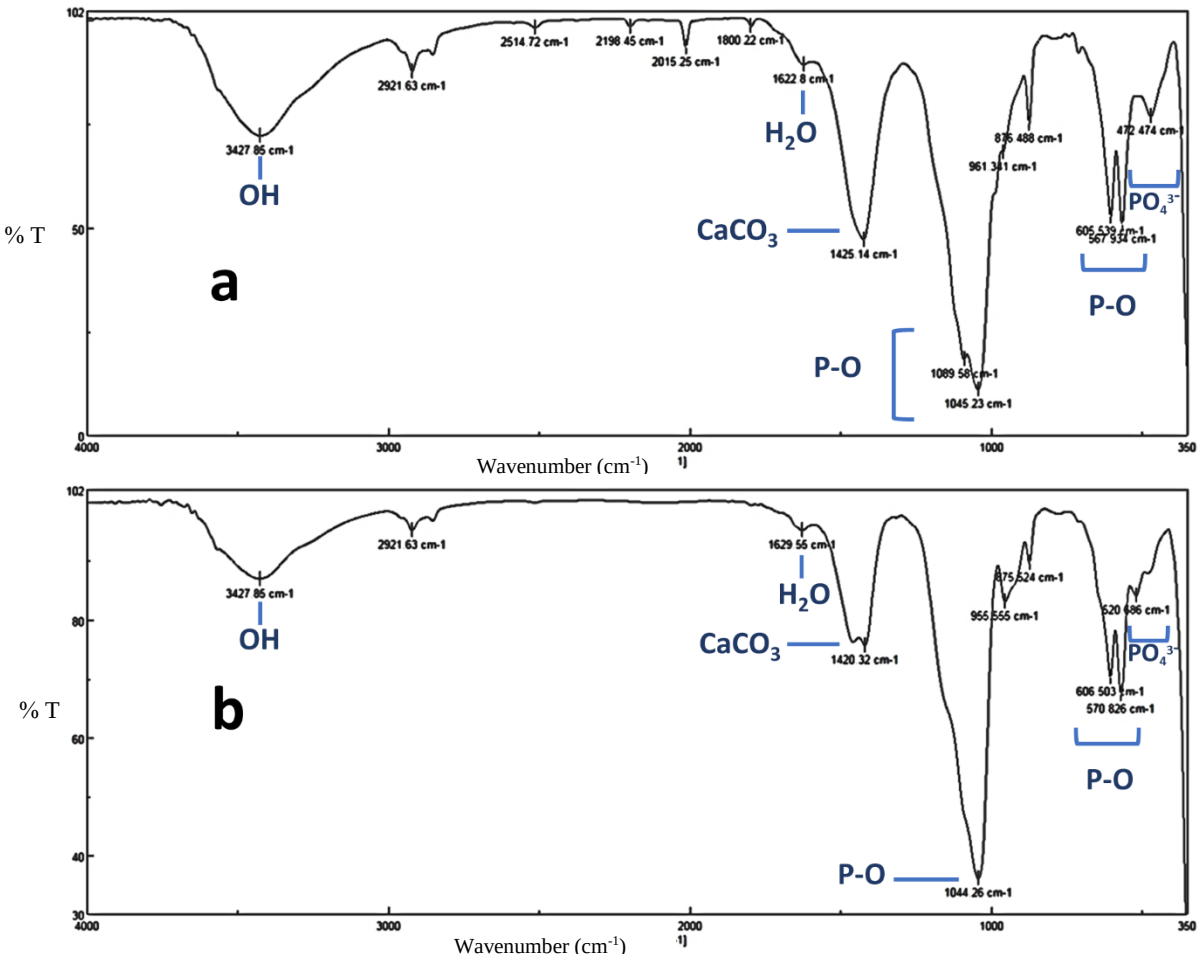

FTIR assignment of pure HA	Spectral assignments group	PO_4^{3-}	OH	$CaCO_3$	H_2O
	Wave number cm^{-1}	1000-1100, 400-700	3400-3600	1400-1500	1600-1650

Figure 3. Fourier transform infrared spectroscopy spectra of the biosynthesized hydroxyapatite of (a) *Bacillus coagulans* and (b) *Bacillus subtilis*

3.4. Assessment of calcium to phosphorus ratio of the synthesized nanocrystals

3.5. Energy-dispersive X-ray analysis

Elemental composition and Ca/P ratios of the sintered samples were assessed using EDX analysis on weight and atomic basis (Figures 6 a,b). The Ca/P ratios of the synthesized nanoparticles from *B. coagulans* were 3.5 and 2.7. These were respectively 4.08 and 3.1 for *B. subtilis* in weight and atomic basis. In commercial HA, the Ca/P stoichiometric ratio is 1.7-2 [26]. High ratios in the biosynthesized nano-HA by *B. subtilis* might be due to the presence of calcite and decomposed calcite from heat-treated samples, compared to the commercial samples, particularly. Based on the evidence, calcite is one of the bioceramics involved in osteogenesis and includes numerous uses in medicine and orthopedics [37]. Results from EDX in this study were similar to those other from the previous studies, pointing out that Ca/P ratios of biological HA from animal bones were higher than those of the commercial types [37-39].

3.5.1. The X-ray fluorescence spectroscopy analysis

In this study, XRF was used to carry out quantitative chemical analysis on the biosynthesized materials. As predicted, key components of HA were calcium and phosphorus with slight quantities of other elements. This study also showed a higher ratio of calcium to phosphorus compared to that studies with commercial materials and chemical HA samples did and data were similar to those of EDX analyses. The synthesized HA sample was purified from calcite particle using 200-nm filters for the first time in this study. Despite HA, calcite is soluble and colloid in water [37]. Calcite particles were washed with pure water and passed through membrane filters. Purification of HA was verified using XRF (Table 1).

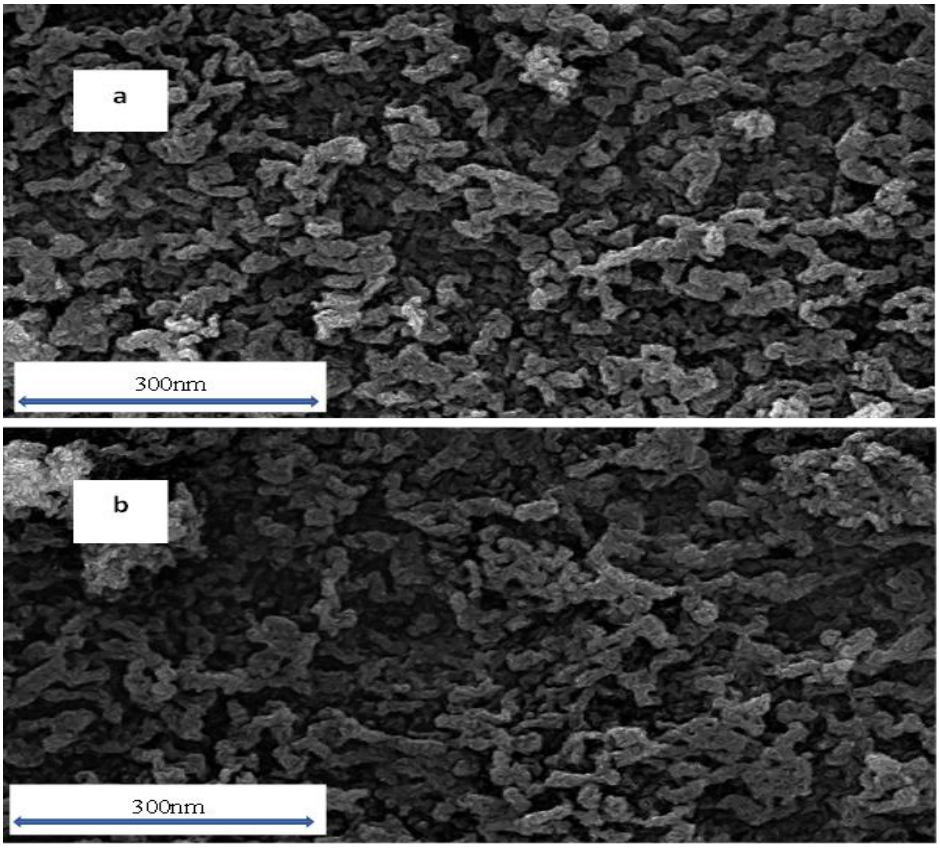

Figure 4. Scanning electron microscope micrographs of the produced bacterial nano-hydroxyapatite from (a) *Bacillus coagulans* and (b) *Bacillus subtilis*

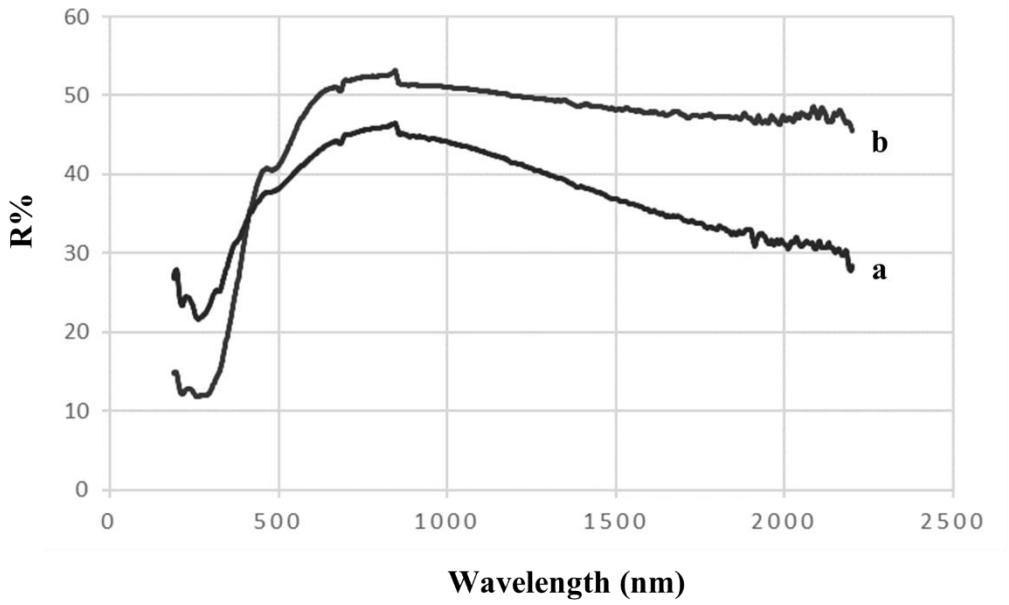

Figure 5. Diffuse reflectance studies of the produced bacterial nano-hydroxyapatite. The UV-vis absorption of the extracted hydroxyapatite from (a) *Bacillus coagulans* and (b) *Bacillus subtilis*

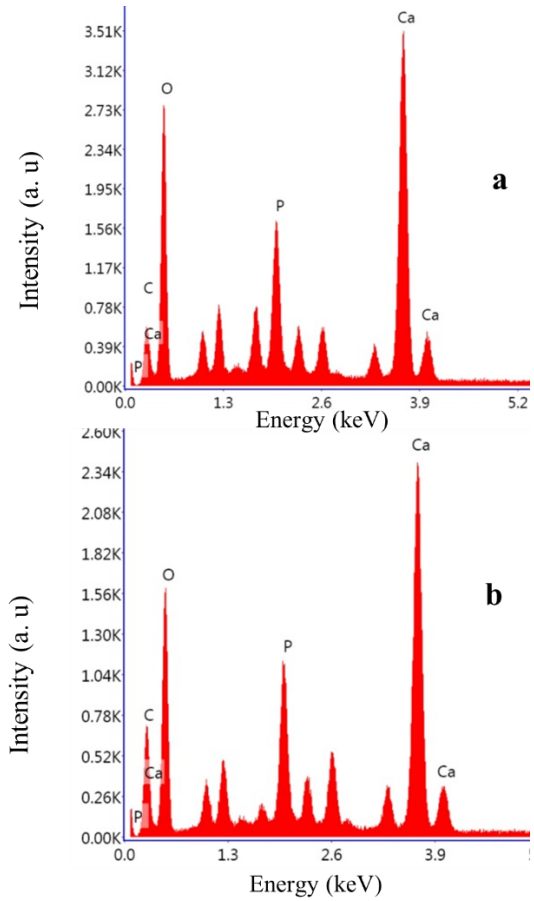

Element	Weight %	Atomic %
C K	0.00	0.00
O K	57.26	75.92
P K	9.36	6.41
Ca K	33.37	17.66

Element	Weight %	Atomic %
C K	3.48	6.13
O K	52.31	69.18
P K	8.70	5.94
Ca K	35.51	18.75

Figure 6. Energy-dispersive X-ray analysis of the sintered nano-hydroxyapatite and chemical weight and atomic composition of (a) *Bacillus coagulans*, (b) *Bacillus subtilis*

Table 1. The X-ray fluorescence elemental composition analysis of the biosynthesized hydroxyapatite before and after nanofilter purification

Elements	Elemental Concentration (% w w^{-1})			
	Sintered HA from *Bacillus coagulans*	Sintered HA from *Bacillus subtilis*	Purified HA from *Bacillus coagulans*	Purified HA from *Bacillus coagulans*
Calcium	48.4	42.90	51.59	62.61
Phosphorus	16.4	8.05	28.50	20.71
Potassium	9.91	15.20	2.51	1.50
Chlorine	8.39	20.60	0.46	0.83
Magnesium	5.11	2.96	4.73	3.41
Sulfur	4.09	4.51	0.93	0.84
Sodium	3.00	2.19	3.50	2.00
Silicon	2.36	1.37	3.31	2.88
Iron	1.08	1.12	2.36	3.05
Manganese	0.62	0.44	0.63	0.61
Copper	0.19	0.19	0.29	0.43
Chromium	0.18	0.21	0.56	0.51
Zinc	0.14	0.14	0.24	0.35
Aluminum	0.12	0.08	0.24	0.32

Data in Table 1 showed that the ratio of Ca/P after filtration respectively decreased from 5.3 to 3 and 2.9 to 1.8 from *B. subtilis* and *B. coagulans*, which were similar to the stoichiometric ratio of commercial HA, especially for *B. coagulans*. Elemental analysis results of biological HA from biological sources of animal bones and plants showed a higher Ca/P ratio than the stoichiometric ratio (e.g. 1.8) [38,39], similar to pre-purification results in the present study. However, XRF analyses carry out for chemically synthesized HA almost showed a ratio of 1.8 [3]. Up-to-date, XRF analysis was not carry out for the synthesized HA by bacteria. In addition to calcium and phosphorus, the synthesized nanoparticles contained small quantities of other elements such as silicon, magnesium, sodium, potassium and zinc as well as other elementals, which the bacteria might use from the culture media. Previous findings showed synthesis

of HA from natural sources with other trace elements [38,39]. Natural human bone-derived HA includes a slight proportion of trace elements, which is the advantage of biological synthesis [19].

3.6. Effects of enzymes on nanoparticle production

Phosphatase activity in *B. coagulans* and *B. subtilis* was detected in all three media such as NA, PVK, and PVK and urea. Data showed that the production of this enzyme in the two strains was quite natural and permanent. Results of the spectrophotometry absorption showed that the quantity of ALP enzyme in the two strains was higher in PVK and urea media, especially in *B. coagulans*. Results of phosphatase activity are shown in Figure 7.Based on the previous reports, *Bacillus* species include an enzymatic activity up to 11 U l^{-1} in the presence of insoluble phosphate; as shown in the current study [24]. A qualitative urease test showed that the two strains were urease positive. After culturing on the surface of a urea-based agar media, bacteria produced ammonia by producing urease, resulting in alkalization of the environment. As a result of the presence of phenol red, the initial yellow environment turned pink during this process. Results showed that HA could only be synthesized in the presence of tricalcium phosphate and urea, while calcite can only be synthesized in the presence of tricalcium phosphate and addition of urea to media does not affect the calcite synthesis.

Synthesis of the HA at nanoscales has been reported for several ALP-producing bacteria [35]. Indeed, it is documented that phosphatase and urease-positive bacteria can biomineralize inorganic crystals such as calcite and HA [22]. Urease-positive *Bhargavaea cecembensis* was able to synthesize calcite as well [25]. Enzymatic synthesis of calcium phosphate nanocrystals by phosphatase and urease has been reported. Based on that reports, alkalinity affects production of HA [40]. Calcite formation in bacteria includes stablished mechanisms and is a result of the interaction in functional groups and calcium ions present in the environment. Functional groups such as carboxylic acids, hydroxyl groups, amino groups, sulfate and sulfhydryl groups deprotonate due to increases in pH, which results in an overall negative charge of extrapolysaccharides produced by the cells, enabling their binding to cationic ions [25]. Synthesis mechanism of HA by urease and phosphatase enzymes in bacteria has not been reported. However, the mechanism of possible synthesis could be described for the first time as follows based on the previous findings [22,24,25,27,32,39-42]. Calcium-binding proteins in the *Bacillus* membrane tend to bind to calcium with significant energy. The Ca-binding protein in the membrane of *Bacillus* absorbs tricalcium phosphate from the media and provides the essential ions for the formation of HA crystals. Calcium-binding protein can possibly activate ALP, which decreases tricalcium phosphate by absorbing insoluble phosphate. Hence, ALP provides phosphate ions for HA formation. Urease is a key enzyme in the process of HA formation by releasing ammonia in culture media and providing alkaline conditions for nano-calcite and HA synthesis. This enzyme manages the binding of calcium ions to phosphate in the HA crystal structure. Eventually, HA synthesizes in the membrane of bacteria. Then, the synthesized crystalline HA from the calcium-binding position binds to teichoic acid with a negative charge. Since the teichoic acid includes an indented serrate structure, HA crystals form woven and turn to braided morphology.

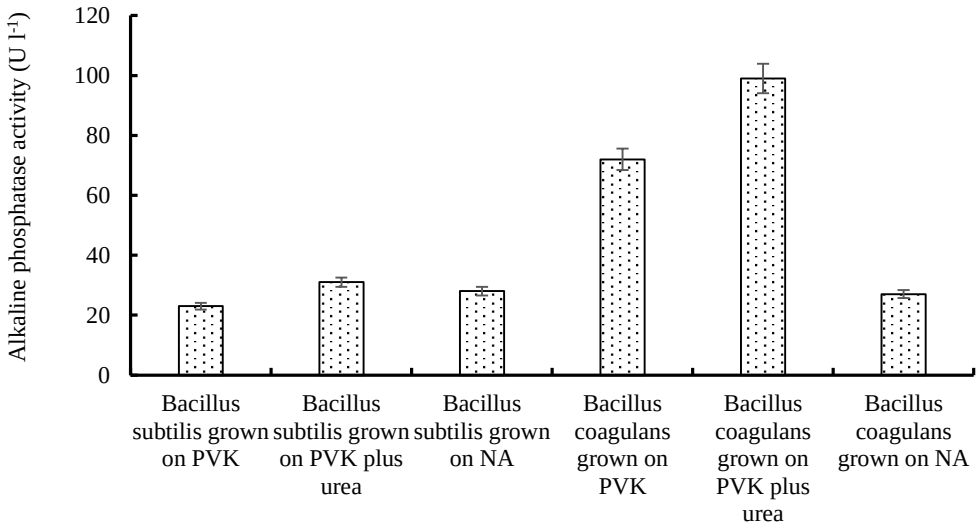

Figure 7: Phosphatase activities of *Bacillus subtilis* and *Bacillus coagulans* strains in various media of Pikovskaya, Pikovskaya and urea, and nutrient agar (NA)

4. Conclusion

In this study, biosynthesis of microbial nano-HA and nano-calcite by *B. coagulans* and *B. subtilis* was carry out using calcium and phosphorous precursors.

The ratio of calcium to phosphorus in pure HA for *B. coagulans* was close to that of stoichiometric HA (e.g. 1.8). Synthesis of biological nano-HA and nano-calcite by the probiotic bacteria could provide a novel non-toxic biocompatible composite for various biomedical, food additive and environmental uses.

Nowadays, several food companies add nano-HA to chewing gums, baby formulas and soft drinks. It has been shown that needle-like nano-HA damages lungs and liver; however, toxicity has not been reported for the woven morphology. Formulation of foods is always changing and developing; however by the introduction of nanoparticles, great cares must be taken for the processed foods. It has been suggested that since probiotics are added to the milk and other food products and their usefulness has been verified for many years, production of nano-HA by these bacteria could be an appropriate option for replacing addition of calcite and HA nanoparticles to diets of the elderly people and infants. This is not only compatible with the microbial ecology, it can strengthen bone formation and may be effective in body growth and health.

5. Acknowledgements

The authors wish to thank University of Isfahan for financial support of this study.

6. Conflict of Interest

The authors declare no conflict of interest.

References

1. Avakyan LA, Paramonova EV, Coutinho J, Oberg S, Bystrov VS, Bugaev LA. Optoelectronics and defect levels in hydroxyapatite by first-principles. J Chem Phys. 2018; 148 (15): 154706. https://doi.org/10.1063/1.5025329

2. Santos C, Turiel S, Sousa Gomes P, Costa E, Santos-Silva A, Quadros P, Duarte J, Battistuzzo S, Fernandes MH. Vascular biosafety of commercial hydroxyapatite particles: Discrepancy between blood compatibility assays and endothelial cell behavior. J Nanobiotechnol. 2018; 16 (1): 1-15. https://doi.org/10.1186/s12951-018-0357-y

3. Szczes A, Hołysz L, Chibowski E. Synthesis of hydroxyapatite for biomedical applications. Adv Colloid Interface Sci. 2017; (249): 321-330. https://doi.org/10.1016/j.cis.2017.04.007

4. Cunha CS, Castro PJ, Sousa SC, Pullar RC, Tobaldi DM, Piccirillo C, Pintado MM. Films of chitosan and natural modified hydroxyapatite as effective UV-protecting, biocompatible and antibacterial wound dressings. Int J Biol Macromol. 2020; 15 (159): 1177-1185. https://doi.org/10.1016/j.ijbiomac.2020.05.077

5. Juntavee A, Juntavee N, Hirunmoon P. Remineralization potential of nanohydroxyapatite toothpaste compared with tricalcium phosphate and fluoride toothpaste on artificial carious lesions. Int J Dent. 2021; 2021: 1-14. https://doi.org/10.1155/2021/5588832

6. Malvano F, Montone AM, Capparelli R, Capuano F, Albanese D. Development of a novel active edible coating containing hydroxyapatite for food shelf-life extension. Chem Eng Trans. 2021; 1 (87): 25-30. https://doi.org/10.3303/CET2187005

7. Kwatra B. Calcium and iron absorption: *in vitro* studies. Int J Med Biomed Stud. 2019; (3): 59-61. https://doi.org/10.32553/ijmbs.v3i12.801

8. Esmaeili Khoozani N, Bahrololoom ME, Bagheri R. Modification of a soft drink by adding calcium carbonate nanoparticles to prevent tooth erosion. J Dent Biomater. 2014; 1 (2): 38-44. http://jdb1.sums.ac.ir/article_42524.html

9. Dorozhkin SV. Calcium orthophosphates (CaPo4) and dentistry. Bioceram Dev Appl. 2016; 6 (2): 96. https://doi.org/10.4172/2090-5025.1000096

10 Schoepf JJ, Bi Y, Kidd J, Herckes P, Hristovski K, Westerhoff P. Detection and dissolution of needle-like hydroxyapatite nanomaterials in infant formula. Nano Impact. 2017; (5): 22-28. https://doi.org/10.1016/j.impact.2016.12.007

11. Mohammadabadi MR, El-Tamimy M, Gianello R, Mozafari MR. Supramolecular assemblies of zwitterionic nanoliposome-polynucleotide complexes as gene transfer vectors: Nanolipoplex formulation and *in vitro* characterisation. J Liposome Res. 2009; 19 (2): 105-115. https://doi.org/10.1080/08982100802547326

12. Heidarpour F, Mohammadabadi MR, Zaidul IS, Maherani B, Saari N, Hamid AA, Abas F, Manap MY, Mozafari MR. Use of prebiotics in oral delivery of bioactive compounds: A nanotechnology perspective. Die Pharmazie. 2011; 66 (5): 319-324. https://doi.org/10.1691/ph.2011.0279

13. Mohammadabadi MR, Mozafari MR. Enhanced efficacy and bioavailability of thymoquinone using nanoliposomal dosage form. J Drug Deliv Sci Technol. 2018; (47): 445-453. https://doi.org/10.1016/j.jddst.2018.08.019

14. Zarrabi A, Alipoor Amro Abadi M, Khorasani S, Mohammadabadi MR, Jamshidi A, Torkaman S, Taghavi E, Mozafari MR, Rasti B. Nanoliposomes and tocosomes as multifunctional nanocarriers for the encapsulation of nutraceutical and dietary molecules. Molecules 2020; 25 (3):638-661. https://doi.org/10.3390/molecules25030638

15. Mohammadabadi MR, Mozafari MR. Development of nanoliposome-encapsulated thymoquinone: Evaluation of loading efficiency and particle characterization. J Biopharm. 2019; (11): 39-46.

16. Arnold M, Rajagukguk YV, Gramza-Michałowska A. Functional food for elderly high in antioxidant and chicken eggshell calcium to reduce the risk of osteoporosis-a narrative review. Foods 2021; 10 (3): 656-676. https://doi.org/10.3390/foods10030656

17. DileepKumar VG, Sridhar MS, Aramwit P, Krut'ko VK, Musskaya ON, Glazov IE, Reddy N. A review on the synthesis and properties of hydroxyapatite for biomedical applications. J Biomater Sci Polym Ed. 2021; (3): 1-33. https://doi.org/10.1080/09205063.2021.1980985

18. Sadat-Shojai M, Khorasani MT, Dinpanah-Khoshdargi E, Jamshidi A. Synthesis methods for nanosized hydroxyapatite with diverse structures. Acta Biomater. 2013; 9 (8): 7591-7621. https://doi.org/10.1016/j.actbio.2013.04.012

19. Pemmer B, Roschger A, Wastl A, Hofstaetter JG, Wobrauschek P, Simon R, Thaler HW, Roschger P, Klaushofer K, Streli C.

Spatial distribution of the trace elements zinc, strontium and lead in human bone tissue. Bone. 2013; 5 7(1): 184-193. https://doi.org/10.1016/j.bone.2013.07.038

20. Saratale RG, Karuppusamy I, Saratale GD, Pugazhendhi A, Kumar G, Park Y, Ghodake GS, Bharagava RN, Banu JR, Shin HS. A comprehensive review on green nanomaterials using biological systems: Recent perception and their future applications. Colloids Surf B Biointer. 2018; (170): 20-35. https://doi.org/10.1016/j.colsurfb.2018.05.045

21. Thackray AC, Sammons RL, Macaskie LE, Yong P, Lugg H, Marquis PM. Bacterial biosynthesis of a calcium phosphate bone-substitute material. J Mater Sci Mater Med. 2004; 15 (4):403-406. https://doi.org/10.1023/B:JMSM.0000021110.07796.6e

22. Ghashghaei S, Emtiazi G. Production of hydroxyapatite nano-particles using tricalcium-phosphate by *Alkanindiges Illinois-ensis*. J Nanomater Mol Nanotechnol. 2013; 2 (5):1-12. https://dx.doi.org/10.4172/2324-8777.1000121

23. Adibpour N, Hosseininezhad, M, Pahlevanlo, A, Hussain, MA. A review on *Bacillus coagulans* as a spore-forming probiotic. Appl Food Biotechnol. 2019; 6 (2): 91-100. https://doi.org/10.22037/afb.v6i2.23958

24. Abdelgalil SA, Soliman NA, Abo-Zaid GA, Abdel-Fattah YR. Dynamic consolidated bioprocessing for innovative lab-scale production of bacterial alkaline phosphatase from *Bacillus paralicheniformis* strain APSO. Sci Rep. 2021; 11 (1): 1-22. https://doi.org/10.1038/s41598-021-85207-4

25. Fabiano V, Indrio F, Verduci E, Calcaterra V, Pop TL, Mari A, Zuccotti GV, Cullu Cokugras F, Pettoello-Mantovani M, Goulet O. Term infant formulas influencing gut microbiota: An overview. Nutrients. 2021; 13 (12): 4225-4236. https://doi.org/10.3390/nu13124200

26. Kamitakahara M, Ohtsuki C, Miyazaki T. Behavior of ceramic biomaterials derived from tricalcium phosphate in physio-logical condition. J Biomater Appl. 2008; 23 (3): 197-212. https://doi.org/10.1177/0885328208096798

27. Eksiri M, Nateghi L, Rahmani A. Production of probiotic drink using pussy willow and echium amoenum extracts. Appl Food Biotechnol. 2017; 4 (3): 155-165. https://doi.org/10.22037/afb.v4i3.16433

28. Bustamante M, Oomah BD, Mosi-Roa Y, Rubilar M, Burgos-Diaz C. Probiotics as an adjunct therapy for the treatment of halitosis, dental caries and periodontitis. Probiotics Antimicrob Proteins. 2020; 12 (2): 325-334. https://doi.org/10.1007/s12602-019-9521-4

29. Odusote JK, Danyuo Y, Baruwa AD, Azeez AA. Synthesis and characterization of hydroxyapatite from bovine bone for production of dental implants. J Appl Biomater Funct Mater. 2019; 17 (2): 1-7. https://doi.org/10.1177/2280800019836829

30. Elbasuney S. Green synthesis of hydroxyapatite nanoparticles with controlled morphologies and surface properties toward biomedical applications. J Inorg Organomet Polym Mater. 2020; 30 (3): 899-906. https://doi.org/10.1007/s10904-019-01247-4

31. Esmaeilkhanian A, Sharifianjazi F, Abouchenari A, Rouhani A, Parvin N, Irani M. Synthesis and characterization of natural nano-hydroxyapatite derived from turkey femur-bone waste. Appl Biochem Biotechnol. 2019; 189 (3): 919-932. https://doi.org/10.1007/s12010-019-03046-6

32. Rong D, Chen P, Yang Y, Li Q, Wan W, Fang X, Zhang J, Han Z, Tian J, Ouyang J. Fabrication of gelatin/PCL electrospun fiber mat with bone powder and the study of its biocompatibility. J Funct Biomater. 2016; 7 (1): 6. https://doi.org/10.3390/jfb7010006

33. Rossi AL, Barreto IC, Maciel WQ, Rosa FP, Rocha-Leao MH, Werckmann J, Rossi AM, Borojevic R, Farina M. Ultrastructure of regenerated bone mineral surrounding hydroxyapatite-alginate composite and sintered hydroxyapatite. Bone. 2012; 50 (1): 301-310. https://doi.org/10.1016/j.bone.2011.10.022

34. SCCS, Opinion on Hydroxyapatite (nano). European Union Scientific Committee on Consumer Safety: Luxembourg, 2015: 55.

35. Kalaiselvi V, Mathammal R, Vijayakumar S, Vaseeharan B. Microwave assisted green synthesis of hydroxyapatite nanorods using Moringa oleifera flower extract and its antimicrobial applications. Int J Vet Sci. 2018; 6 (2): 286-295. https://doi.org/10.1016/j.ijvsm.2018.08.003

36. Monchau F, Hivart P, Genestie B, Chai F, Descamps M, Hildebrand HF. Calcite as a bone substitute. Comparison with hydroxyapatite and tricalcium phosphate with regard to the osteoblastic activity. Mater Sci Eng C Mater Biol Appl. 2013; 33 (1): 490-498. https://doi.org/10.1016/j.msec.2012.09.019

37. Manoj M, Yuan A. A plant-mediated synthesis of nano-structured hydroxyapatite for biomedical applications: A review. RSC adv. 2020; 10 (67): 40923-40939. https://doi.org/10.1039/D0RA08529D

38. Gandhi AD, Kaviyarasu K, Supraja N, Velmurugan R, Suriyakala G, Babujanarthanam R, Zang Y, Soontarapa K, Almaary KS, Elshikh MS, Chen TW. Annealing dependent synthesis of cyto-compatible nano-silver/calcium hydroxyl-apatite composite for antimicrobial activities. Arab J Chem. 2021; 14 (11): 103404-103414. https://doi.org/10.1016/j.arabjc.2021.103404

39. Mostaghaci B, Fathi MH, Sheikh-Zeinoddin M, Soleimanian-Zad S. Bacterial synthesis of nanostructured hydroxyapatite using *Serratia marcescens* PTCC 1187. Int J Nanotechnol. 2009; 6 (10-11): 1015-1030. https://doi.org/10.1504/IJNT.2009.027564

40. Elmi F, Etemadifar Z, Emtiazi G. Biosynthesis of calcite nanocrystal by a novel polyextremophile *bhargavaea cecem-bensis*-related strain isolated from sandy soil. Microb Ecol. 2022; (21):1-10. https://doi.org/10.1007/s00248-022-01977-y

41. Bayraktar D, Tas AC. Formation of hydroxyapatite precursors at 37° C in urea-and enzyme urease-containing body fluids. J Mater Sci Lett. 2001; 20 (5): 401-403. https://doi.org/10.1023/A:1010929825557

42. Abecasis AB, Serrano M, Alves R, Quintais L, Pereira-Leal JB, Henriques AO. A genomic signature and the identification of new sporulation genes. J Bacteriol. 2013; 195 (9): 2101-2115. http://dx.doi.org/10.1128/JB.02110-12

Research Article
pISSN: 2345-5357
eISSN: 2423-4214
OPEN ACCESS
APPLIED FOOD BIOTECHNOLOGY, 2022, 9 (4):275-286
Journal homepage: www.journals.sbmu.ac.ir/afb

بیوسنتز نانوکلسیت و نانوهیدروکسی آپاتیت توسط باکتری‌های زیست‌یار *باسیلوس سوبتیلیس* و *باسیلوس کوآگولانس*

صابره نوری، رسول روغنیان*، گیتی امتیازی، رسول شفیعی

گروه زیست شناسی سلولی و مولکولی و میکروبیولوژی، دانشکده علوم و صنایع زیستی، دانشگاه اصفهان، اصفهان، ایران.

تاریخچه مقاله

دریافت ۳ جولای ۲۰۲۲
داوری ۱۸ جولای ۲۰۲۲
پذیرش ۳۰ جولای ۲۰۲۲

واژگان کلیدی

- *باسیلوس کوآگولانس*
- *باسیلوس سوبتیلیس*
- کلسیت
- افزودنی غذایی
- هیدروکسی آپاتیت
- زیست‌یار

***نویسنده مسئول**

رسول روغنیان

گروه زیست شناسی سلولی و مولکولی و میکروبیولوژی، دانشکده علوم و صنایع زیستی، دانشگاه اصفهان، اصفهان، ایران.

تلفن: ۰۰۹۸۹۱۳۱۱۷۰۶۶۹+

پست الکترونیک:
rasoul_roghanian@yahoo.co.uk

چکیده

سابقه و هدف: در سال‌های اخیر تولید سبز نانومواد به‌دلیل سازگاری آن‌ها با محیط زیست، نسبت به انواع شیمیایی بیش از پیش مورد توجه قرار گرفته است. هدف این مطالعه بررسی تولید نانومواد توسط زیست‌یارها تعیین ویژگی‌های آن‌ها بوده است.

مواد و روش ها: *باسیلوس سوبتیلیس* و *باسیلوس کوآگولانس* در محیط‌های کشت حاوی کلسیم فسفات نامحلول و اوره کشت داده شدند ، و نانوهیدروکسی آپاتیت و نانو کلسیت تولید شد. تولیدات در سه مرحله مورد بررسی قرار گرفتند. در مرحله اول، ذرات تولید شده بر سطح باکتری‌های خشک شده در دمای محیط بررسی شدند. در مرحله دوم، باکتری‌های خشک شده در درجه حرارت ۶۰۰°C سوزانده شدند. در آخرین مرحله، هیدروکسی آپاتیت با استفاده از نانوفیلترها تخلیص شد. ویژگی‌ها و آنالیز عنصری با استفاده از طیف بینی مادون قرمز تبدیل فوریه[۱]، پراکنش پرتو ایکس[۲] ، طیف بینی ماورای بنفش و مرئی[۳]، پراکندگی انرژی اشعه ایکس و فلورسانس اشعه ایکس مورد مطالعه قرار گرفت.

یافته‌ها و نتیجه‌گیری: نتایج نشان داد که نانوکلسیت و نانوهیدروکسی آپاتیت بافته شده در سطح زیست‌توده[۴] خشک شده باکتری‌ها تنها هنگامی‌که در محیط حاوی کلسیم فسفات نامحلول همراه با اوره و القا شده توسط فسفاتاز و اوره‌آز ساخته شد. حذف مواد آلی با عملیات حرارتی منجر به خلوص ذرات شد. نتایج پراکندگی فلورسانس اشعه ایکس خلوص نانوهیدروکسی آپاتیت را بعد از فیلتر ذرات سوخته نشان داد. نسبت کلسیم به فسفر در نمونه *باسیلوس کوآگولانس* به ۱/۸ رسید که مشابه هیدروکسی آپاتیت استوکیومتری است. از آنجایی‌که این نانومواد از زیست‌یارها[۵] تولید می‌شوند، می‌توانند کاندیدای مناسبی برای استفاده در صنایع غذایی، بهداشتی و پزشکی باشند. نانوهیدروکسی آپاتیت بافته شده می‌تواند جایگزین نوع سوزنی شکل در افزودنی‌های غذایی برای نوزادان و سالمندان به‌دلیل ایمنی بالای آن باشد.

تعارض منافع: نویسندگان اعلام می‌کنند که هیچ نوع تعارض منافعی مرتبط با انتشار این مقاله ندارند.

۱ Fourier transform infrared spectroscopy or FTIR
۲ X-ray diffractometry or XRD
۳ Ultraviolet-visible spectroscopy
۴ Biomass
۵ Probiotics